Supporting Information

Strong, tough and environment-tolerant organohydrogels for flaw-insensitive strain sensing

Yuqing Wang[a], *Zhanqi Liu*[a], *Yuntao Liu*[a], *Jun Yan*[a], *Haidi Wu*[a], *Hechuan Zhang*[a], *Huamin Li*[a], *Junjie Wang*[a], *Huaiguo Xue*[a], *Ling Wang*[b], *Yongqian Shi*[c], *Longcheng Tang*[d], *Pingan Song*[e], *Jiefeng Gao*[a]*

1. Characterization

1.1 Ultraviolet-visible-near infrared spectroscopy

The visible light transmittance of the samples was evaluated by an ultraviolet-visible-near infrared absorption spectrometer (Carry 5000, Varian, USA) with the wavelength from 300 to 800 nm.

1.2 X-ray diffraction (XRD) and differential scanning calorimetry (DSC) measurements

PVA was chemically cross-linked by immersion of the gels in glutaraldehyde solution for 5 min. After the gels were transformed to hydrogels, they were further dried at 37 ℃. The dried samples were cut into circular shapes with a diameter of 25 mm for XRD (XRD-7000, SHIMADZU, Japan) and DSC (DSC8500, Perkin Elmer, USA) measurement. The XRD tests were carried out at a rate of 5^{o} min^{-1} in the range of $5\text{-}80^{o}$. The crystal size is calculated by an equation [$D = k\lambda/(\beta\cos\theta)$], where k is 1 when the crystal shape is considered to be a sphere. λ is the wavelength of X-ray diffraction (λ = 0.154 nm), θ is the Bragg Angle, and β is the full width at the peak half peak. For the DSC measurement, the samples (~10 mg) were placed in a nitrogen atmosphere with a flow rate of 30 ml min^{-1} and heated from 50 ℃ to 250 ℃ at a rate of 20 ℃ min^{-1}. The melting enthalpy was obtained by calculating the area of the melting endothermic transition peaks in the temperature range of 200-250 ℃. The standard melting enthalpy of 100% crystalline PVA was 138.6 J/g. The crystallinity of the samples in the dry state was the ratio of the calculated enthalpy to the standard melting enthalpy (138.6 J/g).

1.3 Scanning electronic microscopy (SEM) measurements

In order to remove glycerol and KI, the gels were immersed in water for 48 h, and the water was changed every 6 h. The obtained hydrogels were frozen with liquid nitrogen for 30 min and further fractured in liquid nitrogen. The PVA aerogel was obtained by freeze-drying with a freeze drier (SCIENTZ-10N). The cross-section of the PVA aerogel was sprayed with a layer of gold and then the microscopic morphology was observed by a SEM (Zeiss Supra55, Germany).

1.4 Rheological measurements

All the samples were cut into cylinders with 25 mm in diameter for rheological tests using a rheometer (DHR-2, TA), and dynamic frequency, oscillatory strain, time and temperature scanning were conducted. Dynamic frequency scanning tests (0.1-100 rad s^{-1}) were performed at a fixed strain (γ = 0.1%). The oscillatory strain scanning test (0.1 to 100%) was carried out at a fixed frequency. The time (t = 0 to 200 s) and temperature (T = 20 to 150 ℃) sweep tests were performed with the ω of 6.28 rad s-1 and γ of 0.1% All the above tests were performed at 25 ℃ to unify the temperature conditions.

2 Mechanical measurements

2.1 Mechanical Property Test

A universal tensile machine (Instron Model 3367, USA) was performed to measure all mechanical properties of the samples. The samples possessed a dumbbell shape with a length of 50 mm and a width of 4 mm, and samples' thickness was determined by a spiral micrometer. The stretching rate was fixed at 50 mm/min (with corresponding to strain rate of 2.5 min^{-1}). For the tensile cycle test, the sample was stretched to 50% strain and cyclically load-unload 1000 times with no time interval between each cycle.

To obtain the tensile set values, samples were stretched to 50% strain, held at 50% tensile strain for 10 min, and then recovered. The lengths of sample before stretching and after releasing were recorded. The tensile set values (ε_{ts}) are calculated according to the following formula:

$$\varepsilon_{ts}=\frac{L_f}{L_0}-1 \quad (1)$$

where L_0 and the L_f is the original length and the final length of sample after stretching and releasing.

2.2 Pure shear test

The fracture energy of the gels was measured by a pure shear test using rectangular splines including notched samples with a notch length half of the sample width and unnotched samples. The unnotched and notched samples were 25 mm in width and 50 mm in length, and the initial distance between the two clamps was about 5 mm, and the thickness of all samples was measured with a micrometer before the test. For a notched sample, its length of the notch is about half the width of the sample (~12 mm). Then, the tensile force-displacement curve of unnotched sample was obtained and the notched sample was stretched to obtain the critical displacement for crack extension, which was named ΔL_c. The tensile force-displacement curve of the unnotched sample is integrated at the same displacement to obtain the fracture energy (Γ) calculated by

$$\Gamma = \frac{W(\Delta L_c)}{A} \quad (1)$$

Where $W(\Delta L_c)$ refers to the work for the unnotched sample to reach ΔL_c, and A is the cross-sectional area of the unnotched sample.

2.3 Stress relaxation test

The notched sample for testing stationary crack resistance was 25 mm in width and 50 mm in length, and its length of the notch parallel to the width was 4 mm. Stress relaxation test was performed by stretching the specimen to a strain of 10% at 50 mm min^{-1} and then recording the stress evolution over time.

2.4 Fatigue tests

A customized mechanical stretcher (FULETEST, China) equipped with a 100 N loading cell was used for all fatigue tests and the samples were cut into rectangular splines (50×10 mm^2) for fatigue tests. A crack of approximately 1 mm parallel to the sample width was introduced in the middle of the spline. And the initial distance between the two clamps is about 20 mm. The crack propagation after continuous cyclic stretching was observed by a digital camera (AF4915ZTL, Dino-Lite) and the crack propagation length was recorded. After N tensile cycles of the unnotched sample at

stretch λ, the energy density W can be calculated from the stress-strain curve of the unnotched sample as follows.

$$W(\lambda,N)=\int_{1}^{\lambda} S\,d\lambda \tag{2}$$

S is the measured stress of the unnotched sample and the energy release rate G of the notched sample can be calculated as

$$G(\lambda,N)=2k(\lambda)\times c(N)\times W(\lambda,N) \tag{3}$$

Where k can be expressed as $k=3/\sqrt{\lambda}$ and c is the crack length of the notched sample in the undeformed state. According to the relationship between crack propagation and energy release rate, the fatigue threshold of the sample was determined by the linear extrapolation. Note that no crack propagation was observed during 30 000 cycles under this fatigue threshold.

3. Ionic conductivity and strain sensing test

The impedance spectroscopy of the samples was measured by an electrochemical workstation (Gamry, USA). The samples were cut into a square sheet with a cross-sectional area of 1×1 cm^2 (denoted as A), and its thickness (denoted as L) was measured and recorded. Then, the samples were sandwiched with two stainless steel sheets, which were connected to the electrodes at both ends of the electrochemical workstation for impedance value (denoted as R). All samples were tested at a fixed voltage of 100 mV and a frequency range of 10^{-2} to 10^{6} Hz. The conductivity (denoted as σ) is calculated using the following formula:

$$\sigma=\frac{L}{RA} \tag{4}$$

The samples were cut into rectangular splines (50×10 mm^2) for strain sensing test. During the strain sensing test, a digital source meter (DMM-4040, Tektronix Technology Co. Ltd., USA) was used to record the real-resistance of the gels during stretching and releasing.

Besides, this work is not about living individuals and does not include collection of individually identifiable private information, therefore, approval from a national or institutional ethics board/committee was not a prerequisite. All these experiments have

received the written consent from the volunteer.

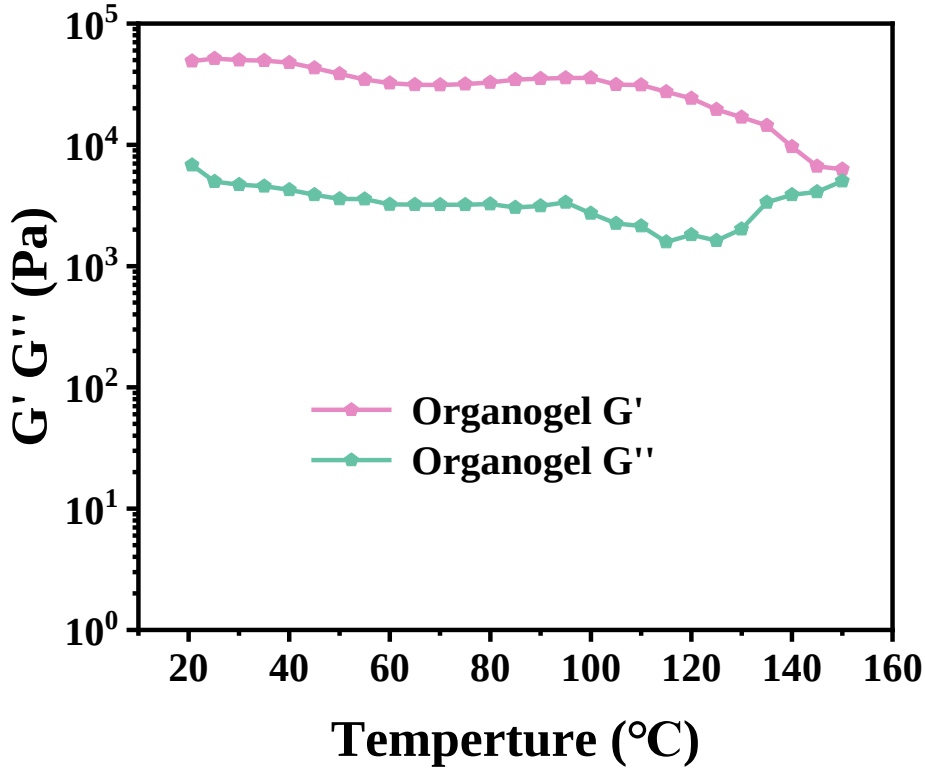

Figure S1. The storage modulus (G') and loss modulus (G'') of PVA/glycerol organogel on a temperature sweep in the range of 20 °C to 150 °C at a strain amplitude (γ) of 0.1% and frequency (ω) of 6.28 rad s^{-1}.

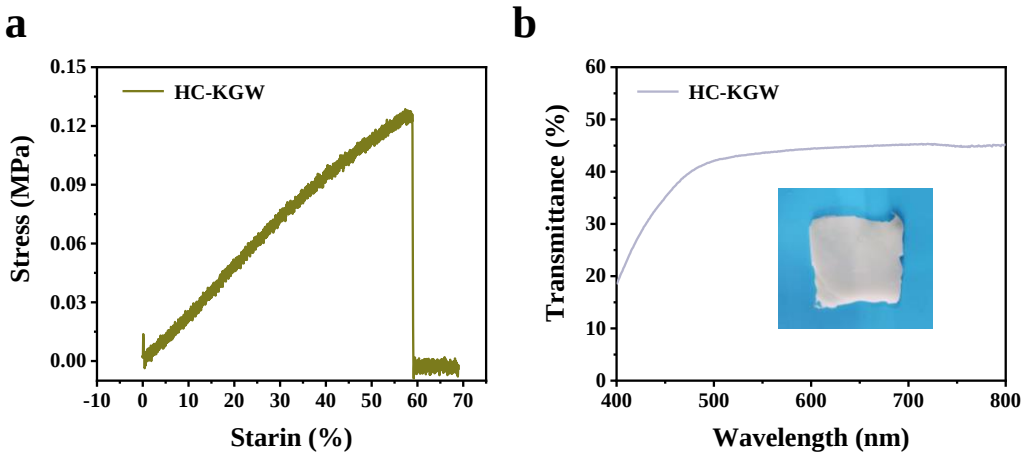

Figure S2. Stress-strain curves and transparency of HC-KGW.

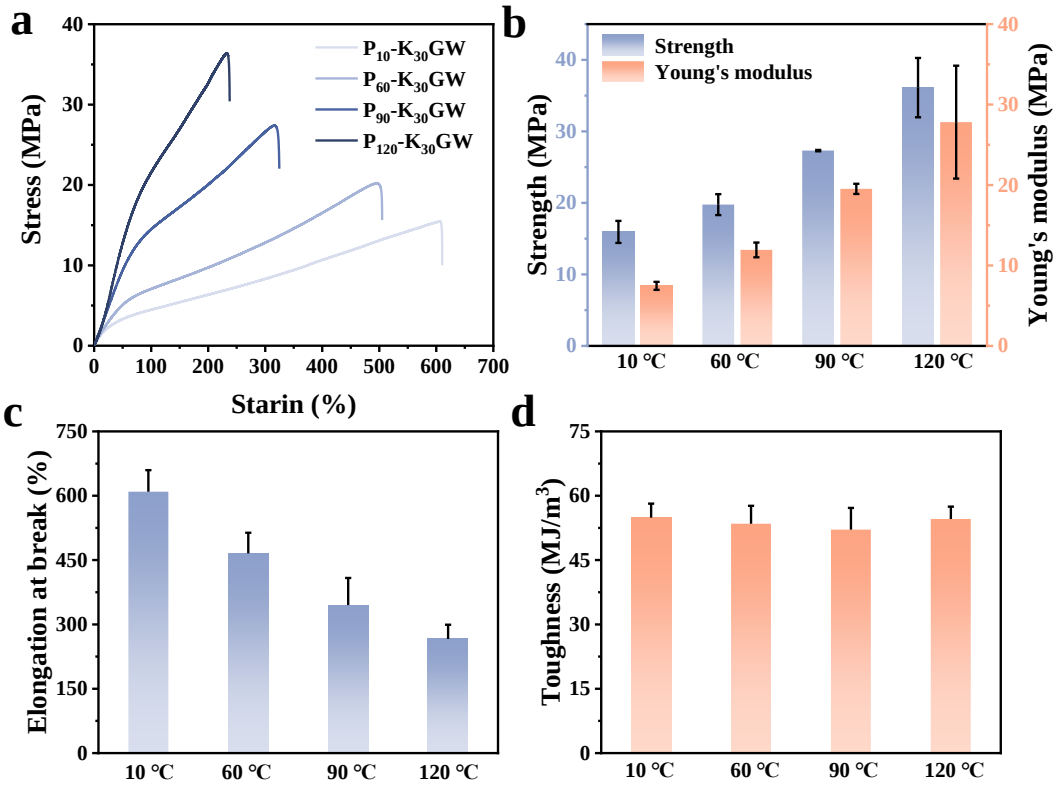

Figure S3. (a) Stress-strain curves of P_x-K_{30}GW and corresponding summary of (b) tensile strength and Young's modules, (c) elongation at break and (d) toughness.

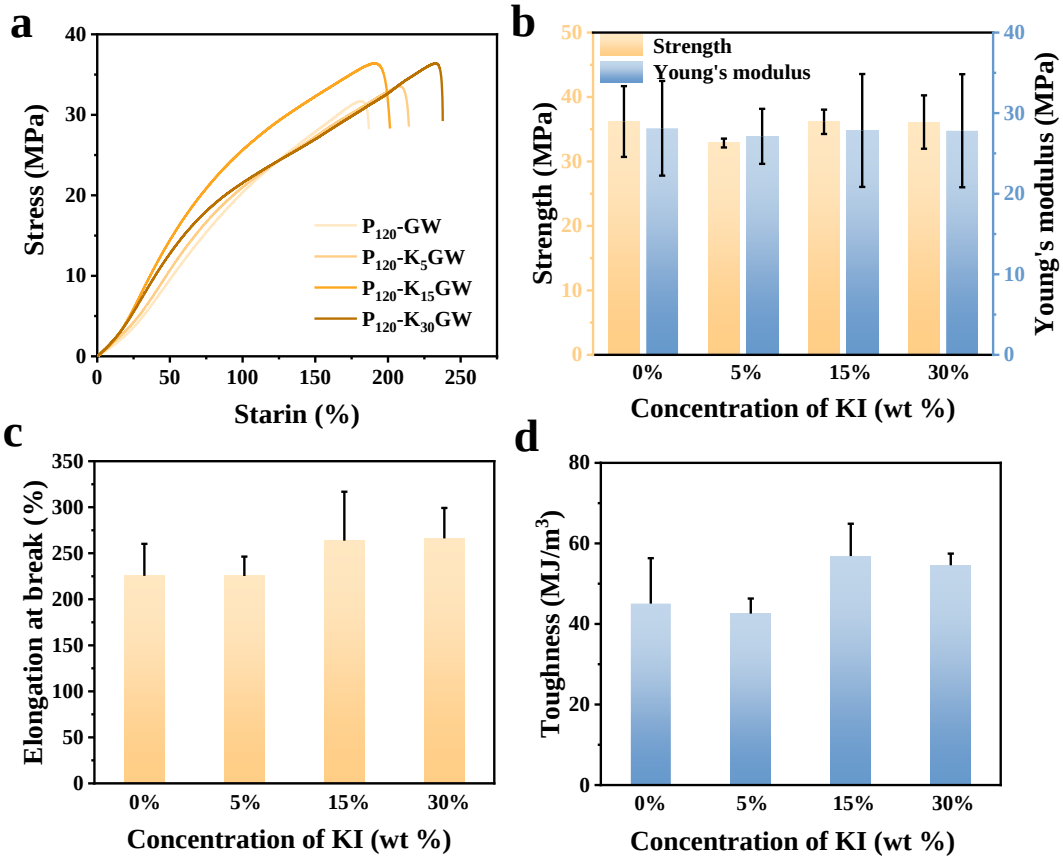

Figure S4. (a) Stress-strain curves of P_{120}-K_yGW and corresponding summary of (b) tensile strength and Young's modules, (c) elongation at break and (d) toughness.

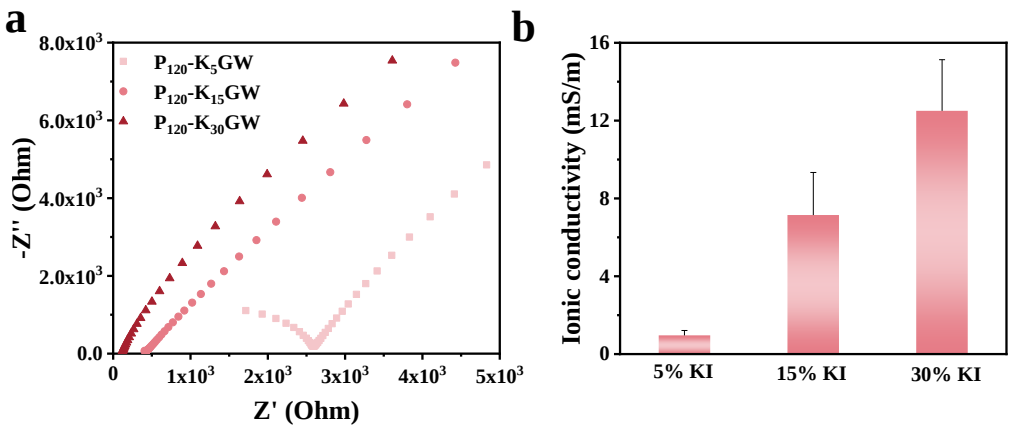

Figure S5. (a) Electrochemical impedance spectroscopy plots of P_{120}-K_yGW and (b) summary of ionic conductivity.

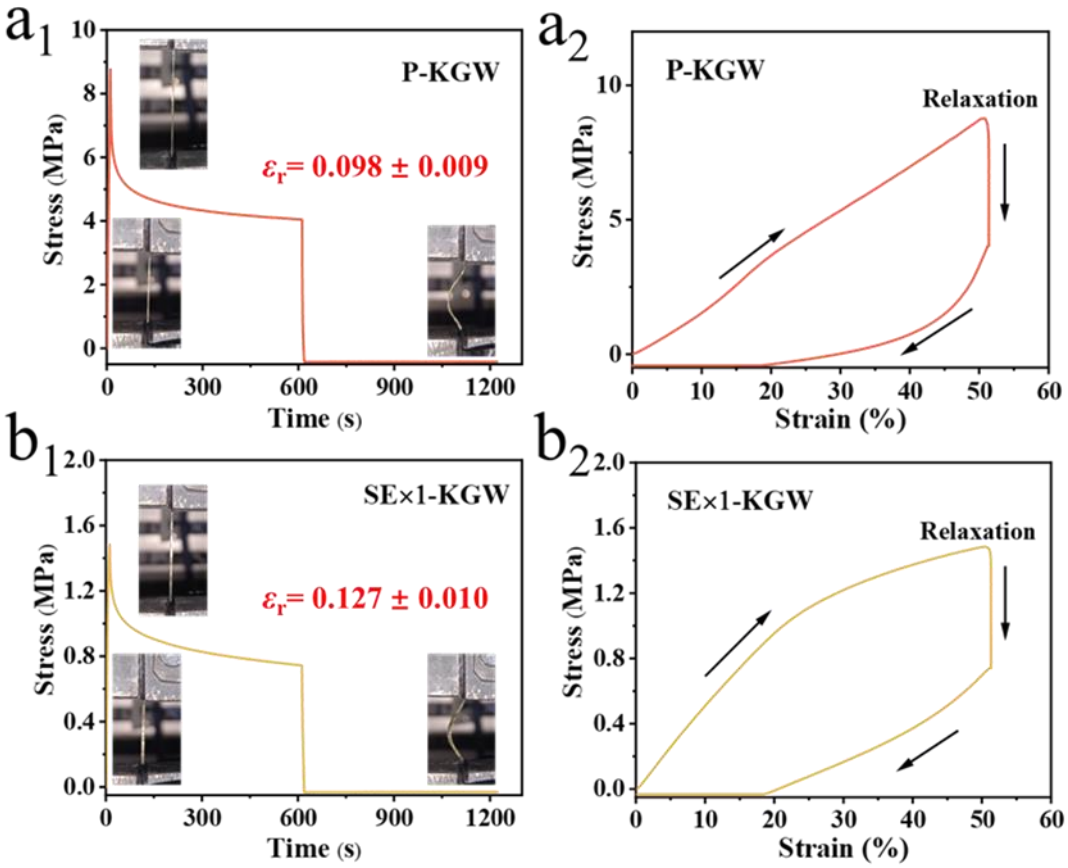

Figure S6. The tensile set values of SE×1-KGW and P-KGW. (a1) Stress-time curve and (a2) stress-strain curve of P-KGW. (b1) Stress-time curve and (b2) stress-strain curve of SE×1-KGW. Insets are the optical images of ICOHs at different stages of stretching, including before stretching, stress retention and stress releasing.

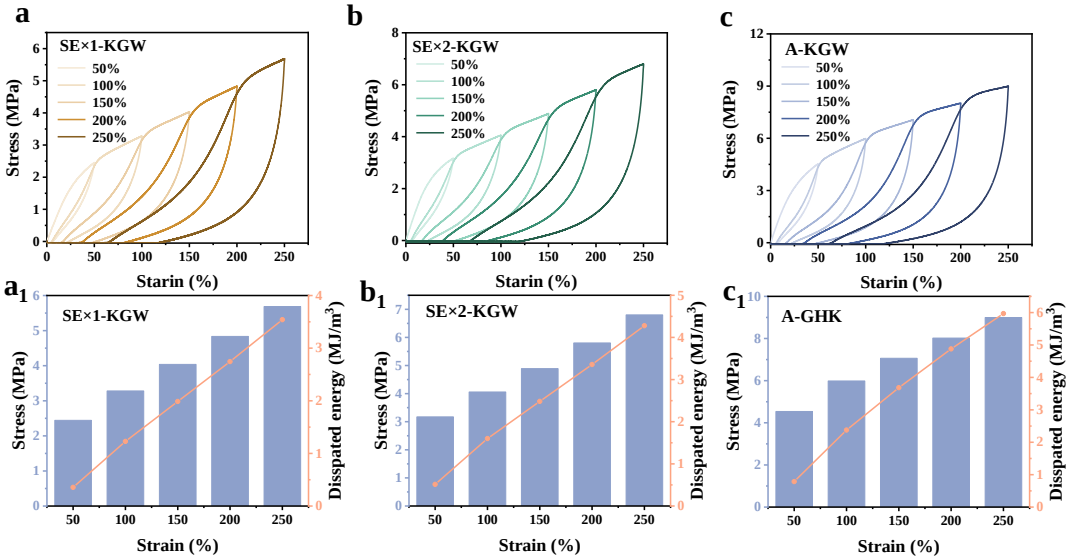

Figure S7. (a-c) Sequential tensile loading-unloading tests without interval under incremental strains, and (a_1-c_1) the corresponding stress and dissipated energy of ICOHs.

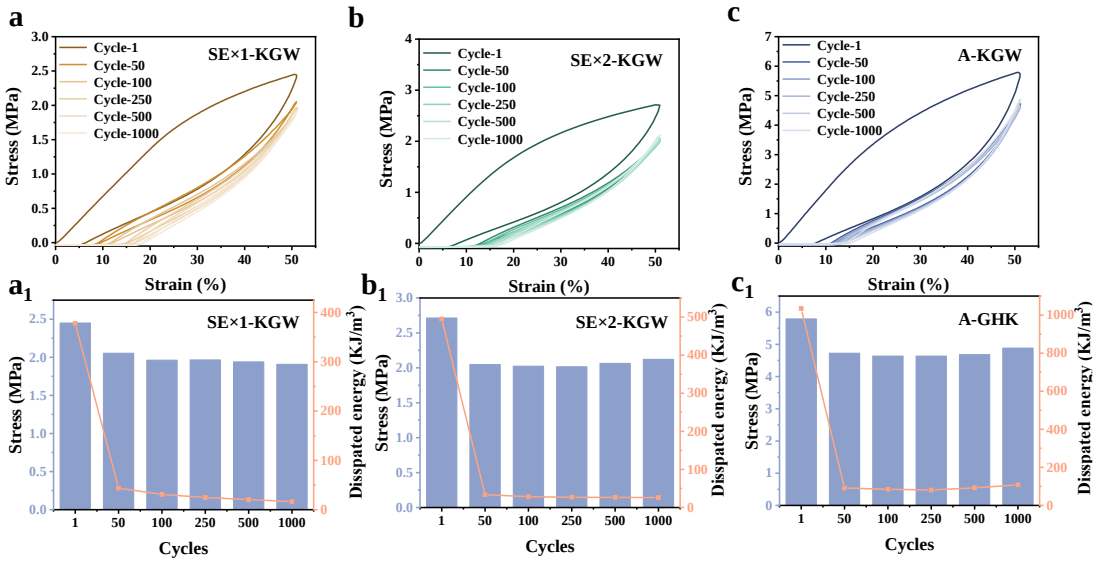

Figure S8. Cyclic tensile stress-strain curves, and the corresponding stress and dissipated energy for the unnotched samples: (a, a_1) SE×1-KGW, (b, b_1) SE×2-KGW, (c, c_1) A-KGW with a fixed strain of 50%.

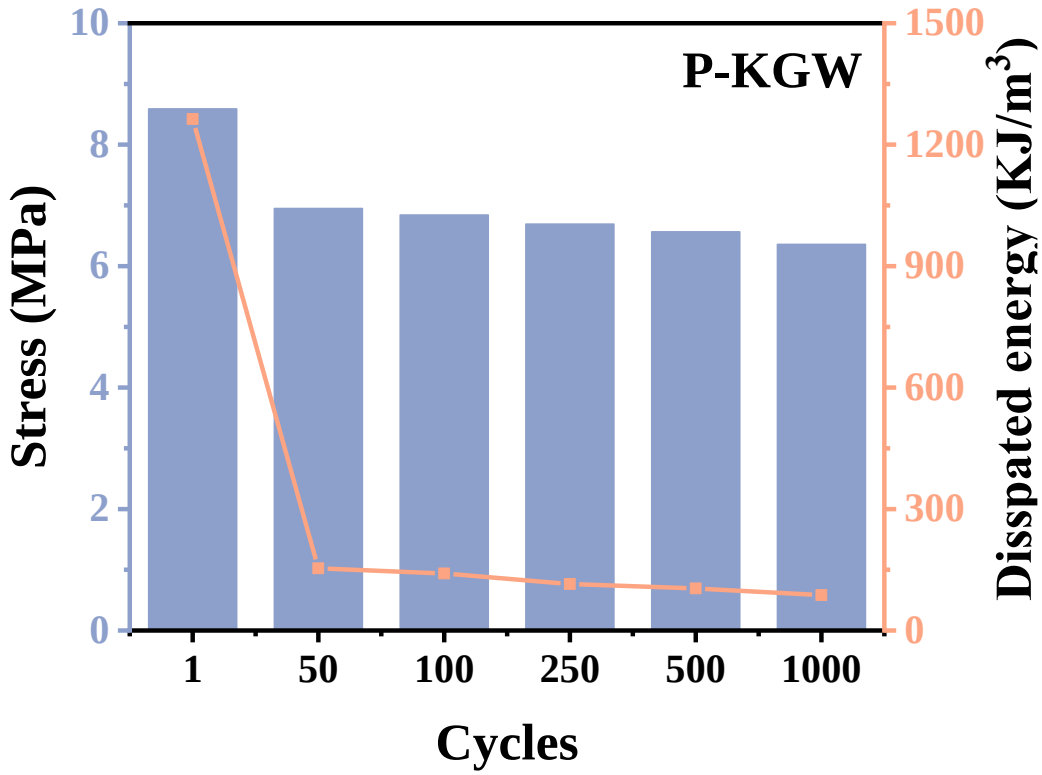

Figure S9. The dissipated energy for of P-KGW with a fixed strain of 50%.

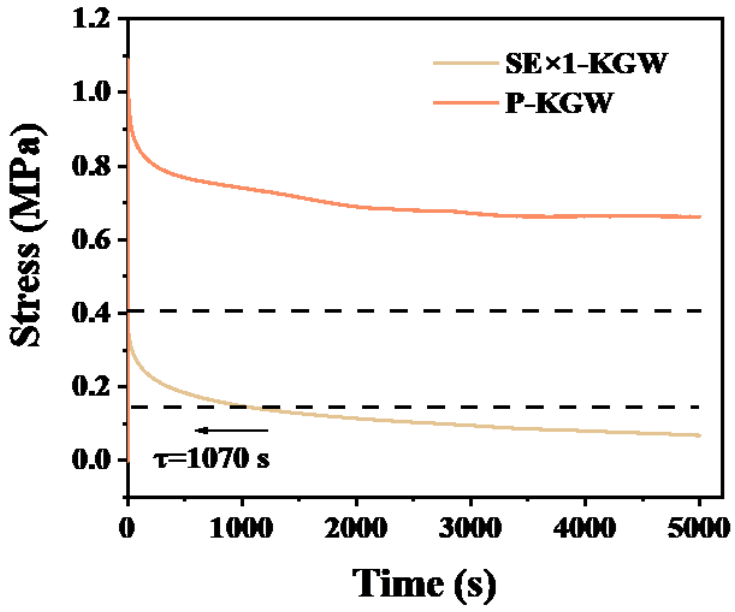

Figure S10. Stationary crack resistance of the notched organohydrogels at 10% strain.

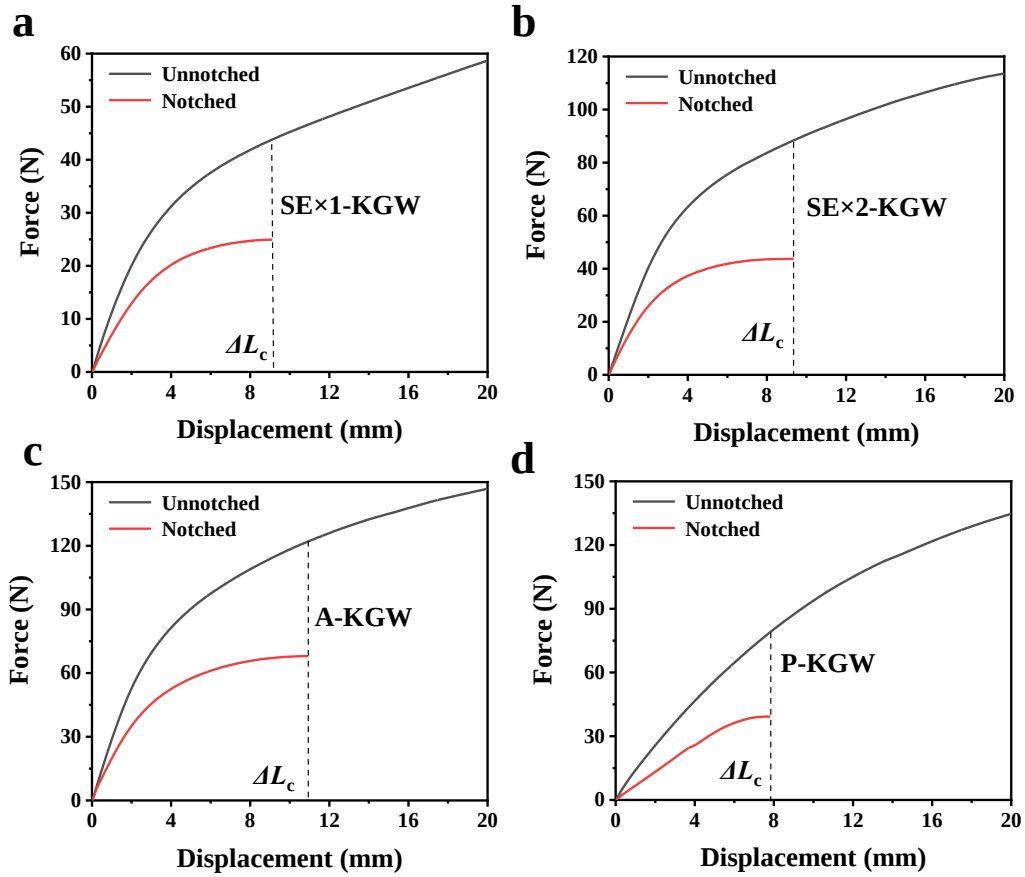

Figure S11. Force-displacement curves of unnotched and notched ICOHs.

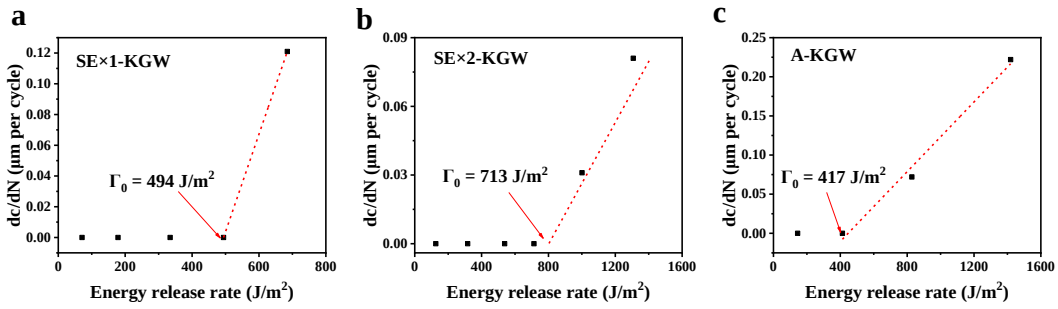

Figure S12. Crack propagation per cycle dc/dN versus applied energy release rate for the notched samples: (a) SE×1-KGW, (b) SE×2-KGW and (c) A-KGW.

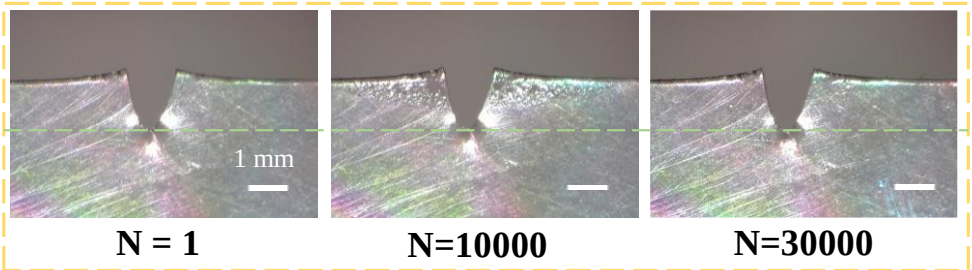

Figure S13. Photographs of the notched sample at the cycle number of 1, 10 000 and 3 0000 for validation of fatigue threshold of P-KGW using the single-notch test.

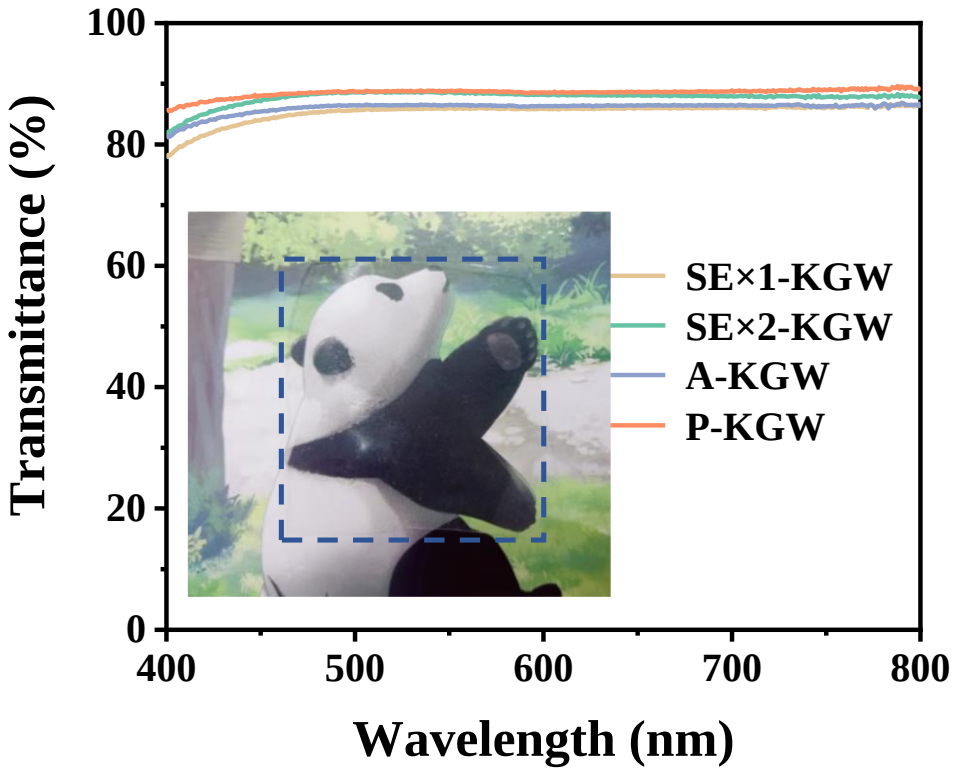

Figure S14. UV-vis transmittance spectra of ICOHs.

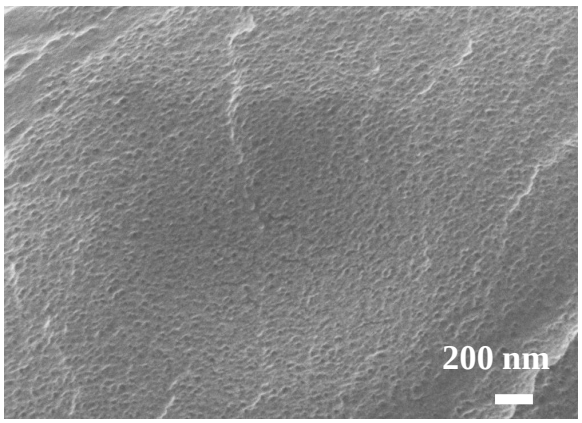

Figure S15. SEM images of A-KGW.

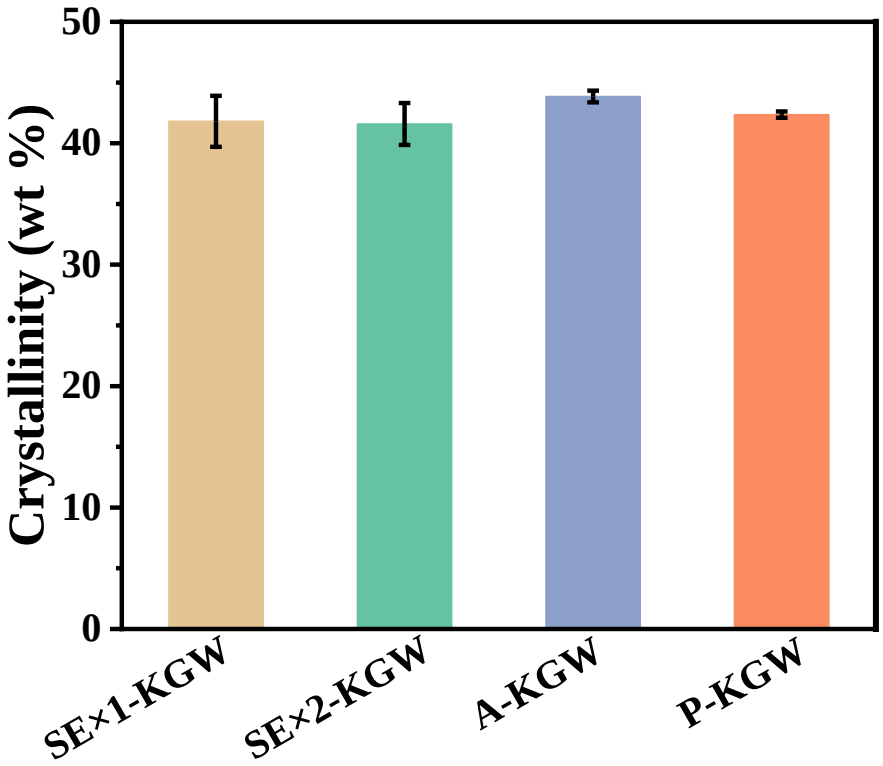

Figure S16. Summary of crystallinity of ICOHs in dry states calculated by DSC tests.

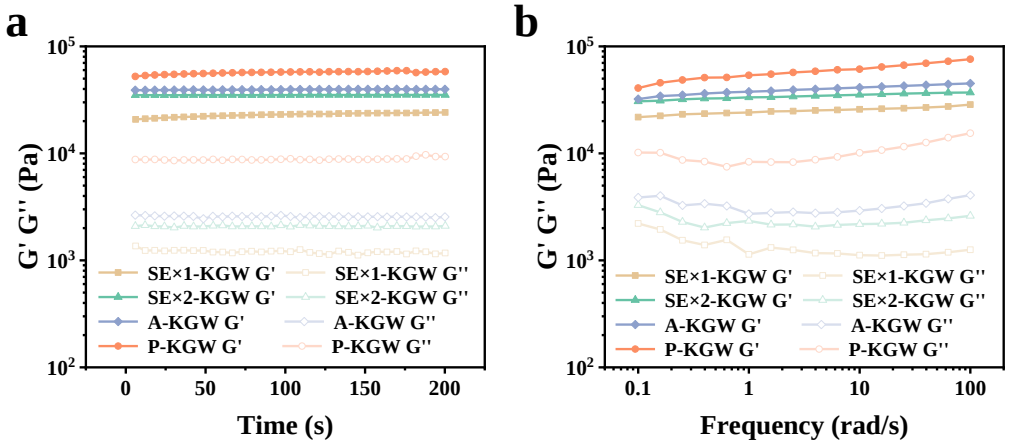

Figure S17. Rheological tests with storage modulus (G') and loss modulus (G'') of ICOHs on (a) time and (b) frequency.

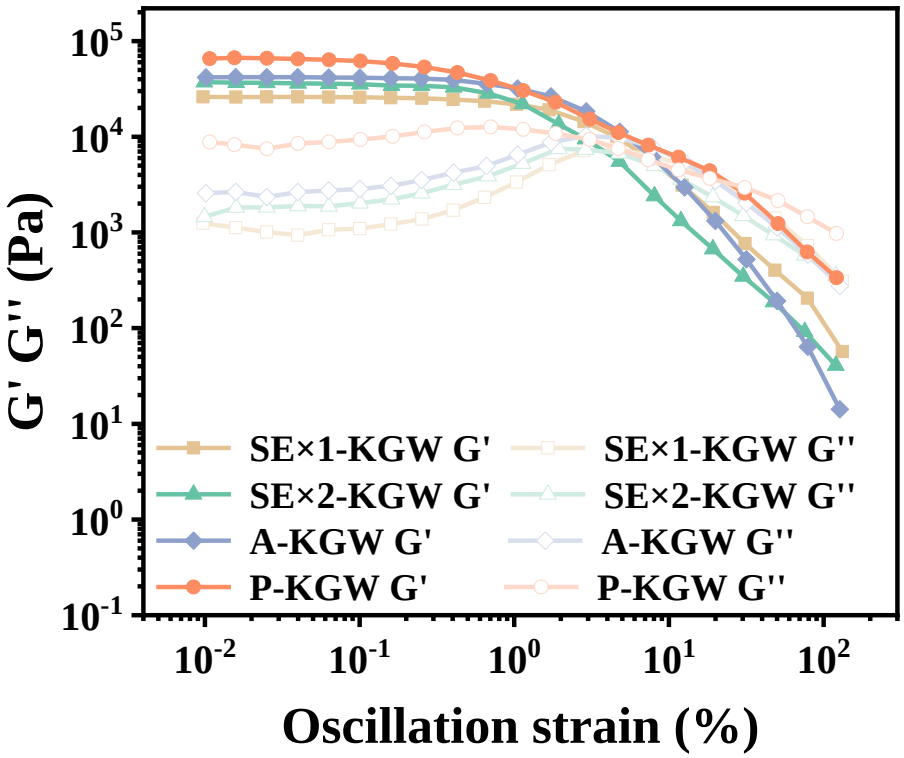

Figure S18. *G′* and loss modulus *G″* of ICOHs as a function of oscillation strain (ω = 6.28 rad s^{-1}, *T*= 25 °C).

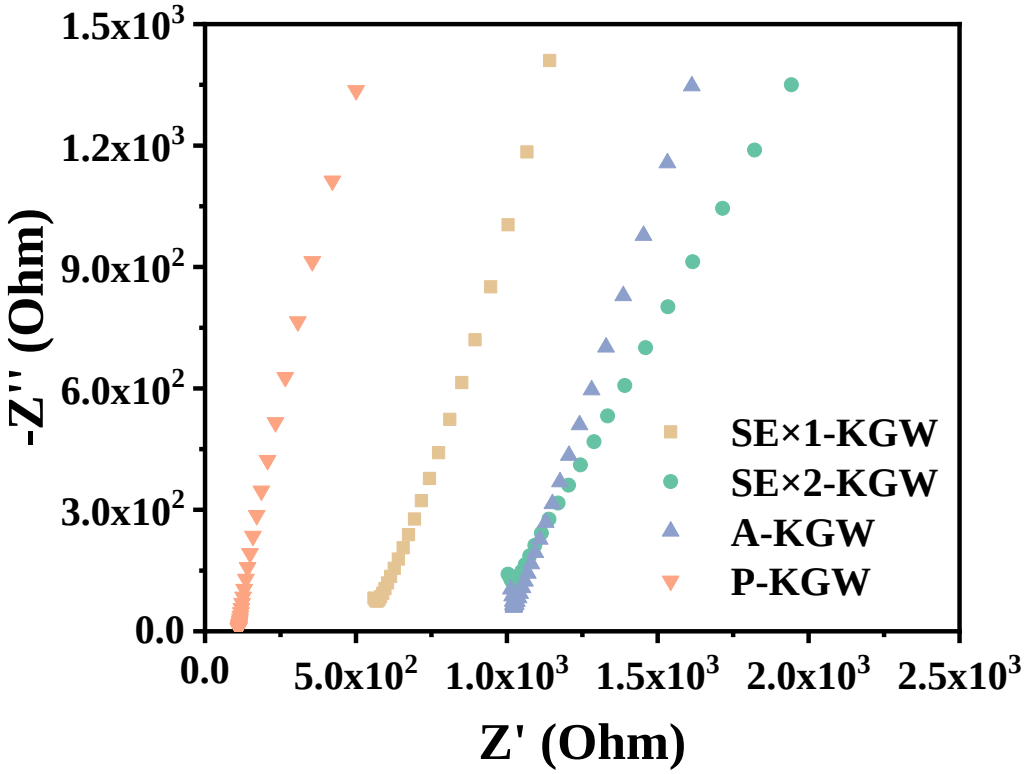

Figure S19. Electrochemical impedance spectroscopy plots of ICOHs.

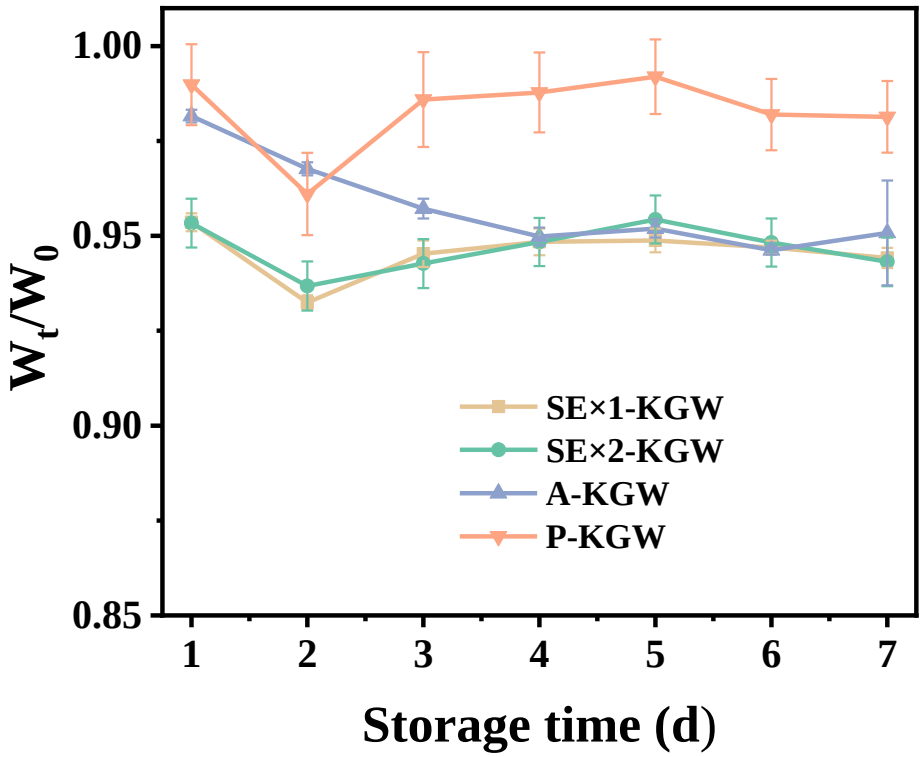

Figure S20. The weight changes of ICOHs in the normal environment for 7 d. W_0 and W_t are the initial weight and the weight in the corresponding storage days of gels.

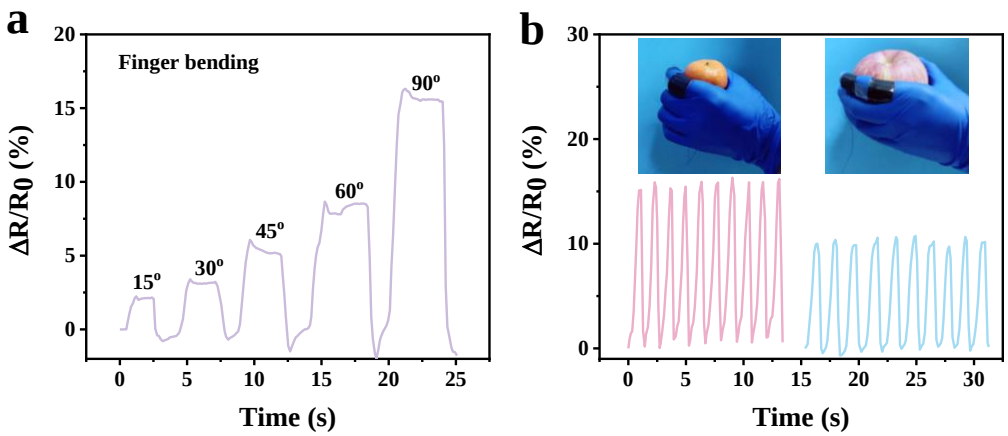

Figure S21. (a) $\Delta R/R_0$ at different angles of finger bending. (b) $\Delta R/R_0$ of holding an orange and an apple.

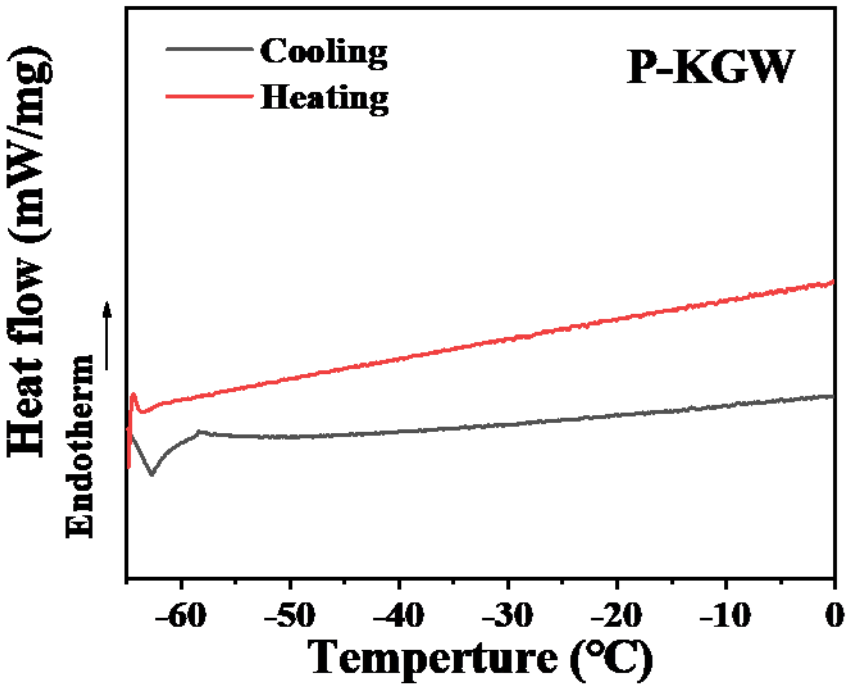

Figure S22. Heat flow curves of P-KGW during the heating and cooling process.

Figure S23. Photograph of P-GHK stretched at −40 ℃.